

Noise-Resilient Point-wise Anomaly Detection in Time Series Using Weak Segment Labels

Yaxuan Wang*
University of California, Santa Cruz
Santa Cruz, CA, USA
ywan1225@ucsc.edu

Hao Cheng*
Hong Kong Baptist University
Hong Kong, China
haocheng@comp.hkbu.edu.hk

Jing Xiong
University of California, Santa Cruz
Santa Cruz, CA, USA
jxiong20@outlook.com

Qingsong Wen
Squirrel AI
Bellevue, WA, USA
qingsongedu@gmail.com

Han Jia
RIPED, CNPC
Beijing, China
hanjia0217@petrochina.com.cn

Ruixuan Song
University of California, Santa Cruz
Santa Cruz, CA, USA
songrx0704@126.com

Liyuan Zhang
DUT & RIPED, CNPC
Dalian & Beijing, China
zhangliyuan@mail.dlut.edu.cn

Zhaowei Zhu
BIAI, ZJUT & D5 Data
Hangzhou, China
zzw@d5data.ai

Yang Liu[†]
University of California, Santa Cruz
Santa Cruz, CA, USA
yangliu@ucsc.edu

Abstract

Detecting anomalies in temporal data has gained significant attention across various real-world applications, aiming to identify unusual events and mitigate potential hazards. In practice, situations often involve a mix of segment-level labels (detected abnormal events with segments of time points) and unlabeled data (undetected events), while the ideal algorithmic outcome should be point-level predictions. Therefore, the huge label information gap between training data and targets makes the task challenging. In this study, we formulate the above imperfect information as noisy labels and propose NRdetector, a noise-resilient framework that incorporates confidence-based sample selection, robust segment-level learning, and data-centric point-level detection for multivariate time series anomaly detection. Particularly, to bridge the information gap between noisy segment-level labels and missing point-level labels, we develop a novel loss function that can effectively mitigate the label noise and consider the temporal features. It encourages the smoothness of consecutive points and the separability of points from segments with different labels. Extensive experiments on real-world multivariate time series datasets with 11 different evaluation metrics demonstrate that NRdetector consistently achieves robust results across multiple real-world datasets, outperforming various baselines adapted to operate in our setting.¹

CCS Concepts

• **Computing methodologies** → **Machine learning**; *Anomaly detect*; • **Mathematics of computing** → *Time series analysis*.

*Both authors contributed equally to this research.

[†]Corresponding author: yangliu@ucsc.edu

¹Code is available at <https://github.com/UCSC-REAL/NRdetector>.



This work is licensed under a Creative Commons Attribution 4.0 International License. *KDD '25, Toronto, ON, Canada*

© 2025 Copyright held by the owner/author(s).

ACM ISBN 979-8-4007-1245-6/25/08

<https://doi.org/10.1145/3690624.3709257>

Keywords

Time Series Anomaly Detection, Positive and Unlabeled Learning, Learning from Noisy Labels

ACM Reference Format:

Yaxuan Wang, Hao Cheng, Jing Xiong, Qingsong Wen, Han Jia, Ruixuan Song, Liyuan Zhang, Zhaowei Zhu, and Yang Liu. 2025. Noise-Resilient Point-wise Anomaly Detection in Time Series Using Weak Segment Labels. In *Proceedings of the 31st ACM SIGKDD Conference on Knowledge Discovery and Data Mining V.1 (KDD '25)*, August 3–7, 2025, Toronto, ON, Canada. ACM, New York, NY, USA, 12 pages. <https://doi.org/10.1145/3690624.3709257>

KDD Availability Link:

The source code of this paper has been made publicly available at <https://doi.org/10.5281/zenodo.14676716>.

1 Introduction

Time series anomaly detection (TSAD) plays a critical role in many real-world monitoring systems and applications, such as robot-assisted systems [37], space exploration [15], and cloud computing [61]. It is the task of discerning unusual or anomalous samples in time series data. Detecting highly anomalous situations is essential for avoiding potential risks and financial losses. Due to the complex temporal dependencies and limited label data, the most dominant research focuses on building the normal patterns from the time series data under an unsupervised setting and can be generalized to unseen anomalies [5, 23, 37, 42, 43, 53, 54, 59]. However, the performance of these unsupervised learning methods is constrained by the lack of prior knowledge concerning true anomalies [10]. They are not good at finding specific anomalous patterns, especially when the anomalies are embedded within the training data for building the normal patterns. An intuitive approach to training a model is through supervised learning, using point-level labels for guidance. However, labeling every anomalous time point is neither practical nor precise due to the significant time and cost required for accurate identification.

Several studies [22, 27] focus on distinguishing anomalous time points from normal ones using segment-level labels for model training. Acquiring weak labels by simply indicating the occurrence of anomalous events is a more practical approach for real-world applications. In the segment-level setup, consecutive time points of a specified length are grouped into a segment, and the labels are provided only for the segment level rather than for individual time points [39, 65]. Specifically, a *positive segment label* indicates that at least one time point within the segment is anomalous, while a *negative segment label* restricts all the points in the segment are normal. One limitation of this setting is that it may overlook potential label errors commonly found in real-world scenarios. In real-world TSAD problems, a positive label can be seen as a true annotation because an observed and recorded abnormal event is often verified. However, the other events may be either normal or abnormal events since the abnormal behavior may be missed. Therefore, detecting point-level anomalies given only segment-level labels with label errors is a practical approach for real-world applications. In this setting, previous methods [22, 27] fail to effectively address the noise within segment-level labels, particularly when abnormal behavior occurs in unverified events.

To overcome the challenges of 1) label errors in segment-level labels and 2) the lack of point-wise labels in TSAD, we propose a two-stage solution:

- **Stage-1: Coarse-grained PU learning:** The coarse-grained segment-level labels are formulated by Positive and Unlabeled (PU) learning [8, 31, 32] problem, i.e., only positive segment labels are provided along with unlabeled segments.
- **Stage-2: Fine-grained abnormal point detection:** We use a data-centric method to score which point is more likely to be abnormal and automatically calculate the best threshold to filter out the abnormal points from a positive segment.

There is a significant information gap between the noisy segment-level labels and the true point-level labels. To bridge this gap when the true point-level labels are missing, we propose a novel loss function that leverages the properties of point-level temporal embeddings to regularize the learning process. Our loss function is motivated by Figure 1, which shows a particular time-series anomaly detection task with *true* point-level labels. The left subfigure shows that abnormal segments are visually distinguishable based on their values in the time series. Moreover, when the true point labels are available, this discriminability is also evident in their temporal embeddings after training, as seen in the range of embedding values in Figure 1(a) (± 20) and Figure 1(b) (± 6). In the meanwhile, there is continuity between consecutive time points in terms of their embeddings in both normal and abnormal segments. The observation motivates us to design a novel loss function in a contrastive fashion, i.e., during training, when the point labels are *missing*, the ideal embedding should also preserve both properties. Therefore, we regularize the temporal embedding to encourage the discriminability between points in segments with different (noisy) labels and the continuity between consecutive points.

Specifically, we introduce NRdetector, a noise-resilient multivariate TSAD framework based on PU learning under inaccurate and inadequate segment-level labels. Our framework includes a coarse-grained PU learning stage followed by a fine-grained abnormal point detection stage. In Stage-1, we first reduce the label noise

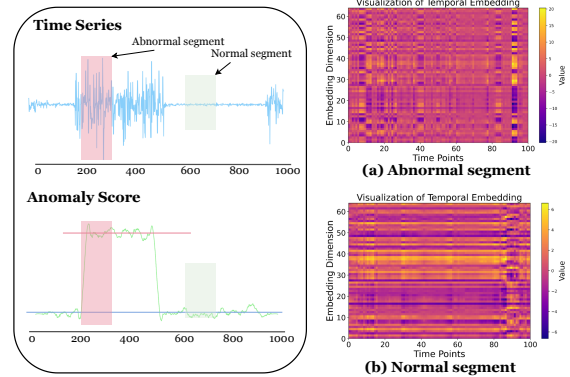


Figure 1: Illustration of the insights. The x-axis in (a) and (b) represents the time step, and the y-axis represents the feature vector. When true point labels are accessible, we observe: a) **Continuity:** The point-level anomaly scores vary smoothly between points within either abnormal (red) or normal (green) segments; b) **Discriminability:** The range of scores (as in the color bar) of anomalous segments (± 20) is sufficiently different from the normal segments (± 6). When point labels are missing, the learned embeddings should also preserve both properties.

rate of the unlabeled set by a confidence-based sample selection module, then apply our designed loss function to guide the segment-level learning and make the output aligned with the time points. In Stage-2, we propose a data-centric point-level detection approach to further determine the point-level anomalies, where the ratio is determined by a training-free automated estimator [68, 69]. Finally, we can get the prediction of all time points. The contributions of this paper are summarized as follows.

- We focus on a novel and practical scenario in TSAD, where abnormal labels are limited and coarse-grained, indicating a time range rather than an exact time point due to challenges like labeling ambiguity or imprecise event timing. To address these issues, we reformulate the problem as a PU learning task and propose NRdetector, a noise-resilient framework designed to handle the imperfect information inherent in this setting.
- To handle the information gap between noisy segment-level labels and missing point-level labels, we propose a new loss function in a contrastive manner, encouraging the smoothness of consecutive points and the separability of points from segments with different labels.
- Experiments on five real-world multivariate time series benchmarks demonstrate that NRdetector consistently surpasses existing TSAD methods in noisy labels setting. We also perform comprehensive ablation studies to evaluate the proposed method.

2 Related Work

Time Series Anomaly Detection. Extensive research has explored TSAD using deep neural networks in unsupervised settings [16, 20, 37, 40, 42, 45, 50, 52, 54, 57, 64]. These methods aim to learn models that accurately describe normality and identify anomalies as deviations from these patterns [55]. However, the lack

of anomaly labels during training makes it challenging to detect different anomalies accurately. Several studies utilize full supervised learning to detect the anomaly time points [4, 11, 41], but obtaining comprehensive point-level labels is impractical due to the labor-intensive nature of data collection. Additionally, label imbalance can hinder supervised model development. Augmentation-based methods [4, 7, 47] can partially address this issue by expanding known anomaly data. Our approach differs from augmentation-based methods by leveraging real, coarse-grained anomaly labels to address a practical setting, whereas those methods rely on synthetic anomalies and typically use window-based slicing, making point-level anomaly determination within each sample unclear. Weakly supervised approaches [22, 27, 44] optimize models to classify segments accurately by leveraging segment-level labels. In this paper, we focus on detecting fine-grained point-level anomalies using partial positive (anomalous) segment-level labels, which allows us to effectively handle real-world scenarios with noisy label information.

Learning with Noisy Labels. In the literature on learning with label noise, popular approaches can be divided into several categories, such as robust loss design [29, 66], transition matrix estimation [38, 68], and sample selection [12]. Among all these methods, the most popular work concentrates on developing risk-consistent strategies, i.e., conducting empirical risk minimization (ERM) with custom-designed loss functions on noisy distributions results in the same minimizer as conducting ERM on the corresponding unseen clean distribution. We aim to train a classifier using a small number of labeled positive examples alongside a larger quantity of unlabeled ones, where the unlabeled data is considered to have noisy labels.

Positive and Unlabeled learning. Positive and Unlabeled (PU) Learning is a special form of semi-supervised learning (SSL). Compared with traditional SSL, this task is much more challenging due to the absence of any known negative labels. Existing PU learning methods typically fall into two categories. The first category involves sample-selection-based approaches, which involve negative sampling from unlabeled data using either handcrafted heuristics or standard SSL techniques [8, 24, 26, 31, 32, 34]. The second category employs a cost-sensitive approach, treating all unlabeled segments as potentially negative and adjusting the objective’s estimation bias through carefully designed misclassification risks [9, 19]. The mainstream of PU methods has shifted towards the framework of cost-sensitive learning [6, 13, 62, 70]. PU Learning has been employed in the field of anomaly detection [39, 58], including time series [34, 60] and video anomaly detection [10, 56]. Our work focuses on segment-level PU learning, where we have partial knowledge of the weak labels for abnormal temporal segments. We consider both sample-selection-based and cost-sensitive approaches to propose a more robust and noise-resilient TSAD detector.

3 Preliminaries

We summarize the key concepts and notations as follows.

3.1 Problem Formulation

We consider a time series anomaly detection problem that aims to identify *anomalous time points* from the *input segments* of temporal

data, where each segment can be collected for a fixed period of time T or obtained by splitting time series into fixed-length temporal data [22]. Formally, given a D -dimensional *input segment* $\hat{X} = [\hat{x}^1, \hat{x}^2, \dots, \hat{x}^T] \in \mathbb{R}^{D \times T}$ of temporal length T , we aim to obtain the point-level anomaly predictions $\hat{y} \in \{0, 1\}$ for each \hat{x}^t , where with $\hat{y} = 0$ for negative (normal) points and $\hat{y} = 1$ for positive (abnormal) points. Let $X \in \mathbb{R}^d$ be the representation vector of the segment \hat{X} , containing the temporal features with d dimensions. Let $Y \in \{0, 1\}$ be the segment-level labels (also as weak labels), indicating if there is at least one anomalous point within the segment. By decoupling the extraction of the time dependency, we could consider the problem as an extremely unbalanced binary classification task (in terms of segment-level predictions) with only partial segment-level positive labels. For detecting the anomaly time points, we need to develop both segment and point-level methods to assign labels to the segments and time points.

3.2 Learning with Noisy Labels

The traditional segment-level TSAD task with clean labels [49] often builds on a set of N training segments denoted by $D := \{(X_n, Y_n)\}_{n \in [N]}$, where $[N] := \{1, 2, \dots, N\}$, X_n is the n -th segment embedding, and Y_n is the label of the n -th segment, which indicates whether anomalous events are observed in the segment. In our considered segment-level classification problem, instead of having access to the clean dataset D , the trained classifier could only obtain a noisy dataset $\tilde{D} := \{(X_n, \tilde{Y}_n)\}_{n \in [N]}$, where the noisy label \tilde{Y}_n may or may not be the same as Y_n . Statistically, the random variable of noisy labels \tilde{Y} can be characterized by transition probabilities [38, 48, 68], i.e., $e_0 := P(\tilde{Y} = 1 | Y = 0)$, $e_1 := P(\tilde{Y} = 0 | Y = 1)$, representing the probability of flipping the clean label $Y = i$ to the noisy label $\tilde{Y} = j$.

3.3 Positive and Unlabeled Learning

Let $p(x, y)$ be the underlying probability density, and $p(x)$ be the marginal distribution of the input. Then the sets of actual positive and negative segments could be denoted as: $\mathcal{X}_P = \{X\}^{N_P} \sim p_P(x)$, and $\mathcal{X}_N = \{X\}^{N_N} \sim p_N(x)$, where $p_P(x)$ and $p_N(x)$ denote the class-conditional distribution of positive and negative segments respectively. The whole training input set $\mathcal{X} = \mathcal{X}_P \cup \mathcal{X}_N = \{X\}^N \sim p(x)$ and the marginal distribution can be formulated as $p(x) = \pi_P \cdot p_P(x) + \pi_N \cdot p_N(x)$, where $N = N_P + N_N$, $\pi_P = P(Y = 1)$ is the class prior probability and $\pi_N = 1 - \pi_P$.

PU learning is a special case, in the way that only a small portion of positive data are labeled. Formally, the input of training set $\mathcal{X}_{PU} = \mathcal{X}_L \cup \mathcal{X}_U$ where \mathcal{X}_L or \mathcal{X}_U represents the labeled positive or the unlabeled subset of both negative and positive segments, respectively. In our paper, we consider the scenario [3] which is practical that positives are labeled uniformly at random and independently of their features, while the unlabeled data are, i.i.d drawn from the real marginal distribution: $\mathcal{X}_L = \{X\}^{N_L} \sim p_P(x)$, $\mathcal{X}_U = \{X\}^{N_U} \sim p_P(x) = p(x)$, where $N = N_L + N_U = N_P + N_N$. Note that the labeled segment set is much smaller than the unlabeled set, that is $N_L \ll N_U$.

The classification task aims to identify a classifier $f \in F : \mathbb{R}^d \rightarrow \mathbb{R}$ that outputs the anomaly score of the segment, where $f(X) \in [0, 1]$. A hyperparameter threshold τ is used to decide if

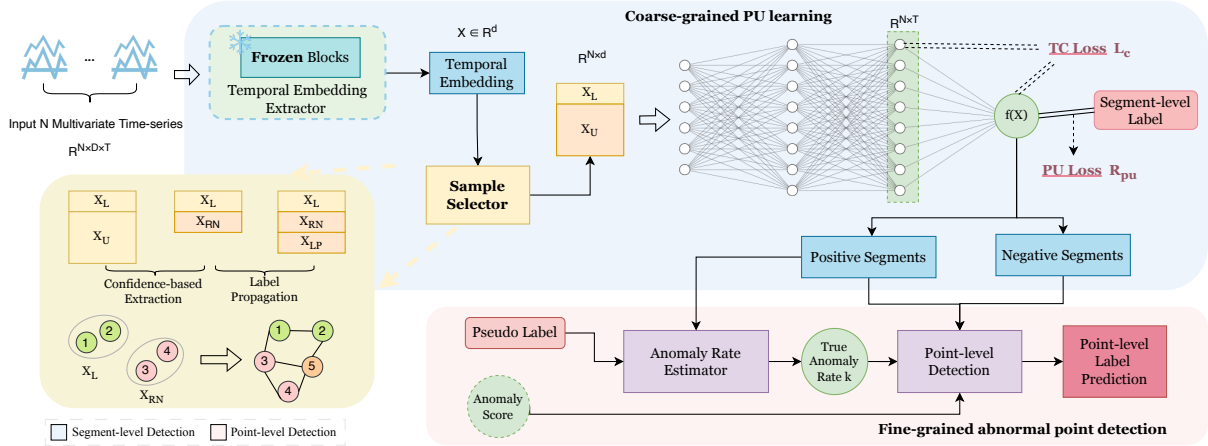


Figure 2: The workflow of the NRdetector framework. NRdetector consists of two main stages: coarse-grained PU learning and fine-grained abnormal point detection. In the Sample Selector module, \mathcal{X}_L denotes the set of labeled positive segments, \mathcal{X}_U denotes the set of unlabeled segments, \mathcal{X}_{RN} denotes the set of extracted reliable negatives based on the confidence scores, and \mathcal{X}_{LP} denotes the set of likely negatives after the label propagation process. $f(X)$ represents the output from the last linear layer of our classifier, processed through a Sigmoid function. TC Loss is the time constraint loss and PU Loss is the non-negative PU risk estimator in Section 4.2.3.

the segment is anomalous ($f(X) > \tau$) or not. Also known as the expected empirical risk:

$$R = \mathbb{E}_{(X,Y) \sim p(x,y)} [\mathbb{1}(\hat{Y}, Y)], \quad (1)$$

with $\hat{Y} \in \{0, 1\}$ denoting the predicted label of segment X by f based on the threshold; $\mathbb{1}(\hat{Y}, Y)$ refers to the 0-1 loss, which equals 0 when $\hat{Y} = Y$ and otherwise 1. One common choice is training a deep neural network (DNN) by minimizing the empirical risk: $\hat{f} = \arg \min_f \frac{1}{N} \sum_{n=1}^N \mathcal{L}(f(X_n), Y_n)$. Notation $\mathcal{L}(\cdot)$ represents the surrogate loss function [2], i.e., cross-entropy loss.

We treat the corresponding dataset of input \mathcal{X}_{PU} as the noisy dataset \tilde{D} of the clean dataset D , thus we can get a special form of the noise transition matrix, where e_0 is equal to 0 in the PU setting. Note that we don't have access to the point-level labels.

4 Methodology

In this section, we introduce a noise-resilient time series anomaly detection approach designed to identify point-level anomalies by leveraging the weak segment labels. Figure 2 illustrates the overall framework of the NRdetector.

4.1 Overall Framework

Our framework includes Stage-1 (confidence-based sample selection and robust segment-level learning) and Stage-2 (data-centric point-level detection). At the initial stage, we extract the Temporal Embedding of the input multivariate time series (Section 4.2.1). The extracted temporal dependencies will be learned through the pre-trained informative representation model. In the sample selection module (Section 4.2.2), we employ the Sample Selector based on the confidence score to identify reliable and likely negative segments before training, aiming to reduce the imbalance between \mathcal{X}_L and

\mathcal{X}_U and lower the proportion of corrupted segment-level labels (actual positive labels) in the training dataset.

In the robust segment-level learning module (Section 4.2.3), the NRdetector employs a six-layer MLP classifier equipped with a specially designed loss function to guide the learning process. In the training process, we just see all selected unlabeled segments as negative (normal), which might result in a negative prediction preference of the classifier. Thus, the PU Criterion module plays a crucial role in our design. It can correct the problem of overfitting the negative segments and consider the temporal feature within the segments.

More specifically, the PU criterion comprising two components: (1) the PU loss, designed to effectively mitigate noise in the segment-level labels and accurately classify input segments according to their anomaly labels; and (2) the Time Constraint (TC) loss, which bridges the gap between noisy segment-level labels and missing point-level labels and also considers temporal features within segments. Note that the temporal segments here are actually a sequence of temporal representations of consecutive time points. Thus, we can ignore the different time series outliers [21], like the point-wise outliers and pattern-wise outliers. Based on this, we know that normal segments tend to share the same latent pattern, while anomalous segments may have different patterns, but there's one stable thing: the pattern inside the segment itself should be consistent. The key insight is that the point-level anomaly scores should vary smoothly between points within one segment. And the average scores of the anomalous segments ought to be greater than those of the normal segments. We can distinguish anomalous segments from normal segments with the well-designed PU Criterion.

After obtaining the segment-level prediction, we propose a data-centric point-level detection approach to further determine the point-level anomalies (Section 4.3).

4.2 Stage-1: Coarse-Grained PU Learning

4.2.1 Temporal Embedding. This module projects the time-series data into the required feature dimensions. To extract temporal features, we utilize the basic architecture of dilated CNN (DiCNN) as introduced by WaveNet [35]. We regard the current unlabeled data as negative and the abnormal data in the labeled data as positive and put it into the WETAS [22] framework. Note that the extractor here can be replaced with another temporal feature extractor [55, 64]. Then, we interpret the model output vector h_t at each point to be a temporal representation of that point. The segment-level temporal embedding is obtained by global average pooling (GAP) [25] on the output vectors along the time axis. Additionally, we determine the anomaly score S of each time point through the use of the anomaly weight $w \in \mathbb{R}^d$ and sigmoid function σ .

$$X = \text{GAP}(h_1, h_2, \dots, h_T) \in \mathbb{R}^d, \quad S = \sigma(w^T X). \quad (2)$$

4.2.2 Sample Selector. To enlarge the differences between the anomalous and normal patterns and reduce the imbalance in the training dataset, we propose a network-based unlabeled negative segments selector based on the confidence scores. This selector identifies the most reliable negative segments within the unlabeled dataset \mathcal{X}_U , which consists of noisy negatives, to create a refined unlabeled dataset but with fewer likely anomalous data. We calculate the confidence scores of each segments in \mathcal{X}_U using the cosine similarity metric. Segments that are most dissimilar to the segments in \mathcal{X}_L will have higher confidence scores. Based on the scores, we formulate a reliable negative segments set \mathcal{X}_{RN} . Following the assumptions presented in [8], we use Katz index [32] to measure the similarity between each segment X . We also created a KNN network, where the segments are represented as nodes. Based on the ideas that the class information of neighboring segments should be similar and the class information of labeled segments assigned during the process must be consistent with known label information (anomalous), we utilize label propagation [8] to minimize the function and obtain the corresponding propagated label F :

$$L(F) = \frac{1}{2} \sum_{X_i, X_j \in \mathcal{X}_L \cup \mathcal{X}_U} w_{X_i, X_j} \Omega(F_{X_i}, F_{X_j}) + \mu \sum_{X_i \in \mathcal{X}_L} \Phi(F_{X_i}, \bar{Y}_{X_i}), \quad (3)$$

where Ω and Φ are distance functions, F is the class information vector, $F \in \mathbb{R}^{N \times 2}$; $F_{X_i}, F_{X_j} \in \mathbb{R}^2$, indicating the propagated label information of certain segments X_i and X_j ; w_{X_i, X_j} is the similarity between X_i and X_j ; \bar{Y}_{X_i} is the given label of positive segments, denoting the vector $[0, 1]$. The detailed algorithms are in Appendix A. By using this algorithm, we can create a new unlabeled dataset $\tilde{\mathcal{X}}_U = \mathcal{X}_{RN} \cup \mathcal{X}_{LP}$ based on F , where \mathcal{X}_{LP} refers to those reliable negatives by the label propagation process.

Intuitively, implementing the selector can reduce the label noise rate while at the cost of losing some training samples. When the benefit of label noise rate reduction is more significant than the harm of losing training samples, the performance can be improved. We defer more analyses to Appendix B.1.

4.2.3 PU Criterion. In the robust segment-level learning module, we formalize a loss function based on the Non-negative Risk Estimator [19] and the designed Time-Constraint Loss, which considers the underlying temporal structure of the anomalous and normal

segments. The last layer of our classifier is the anomaly score $f(X)$ of the segment and the previous layer is the T-dimension output $h(X)$, which can be seen as the anomaly scores of each point within the T-length segment.

Non-negative PU Risk Estimator (PU Loss). In traditional binary classification task, thanks to the availability of \mathcal{X}_P and \mathcal{X}_N , $R(f)$ can be approximated directly by:

$$R(f) = \pi_P \cdot \mathbb{E}_{X \sim p_P(x)} [\ell(f(X), 1)] + \pi_N \cdot \mathbb{E}_{X \sim p_N(x)} [\ell(f(X), 0)] \quad (4)$$

where ℓ is by default the 0-1 loss ℓ_{01} ; when used for training, ℓ_{01} is replaced with a surrogate loss. Based on distribution alignment [62], i.e., $\mathbb{E}_{(X,Y) \sim p_P(x,y)} Y = \pi_P$, we can formulate the optimization objective as follows:

$$R_{pu} = 2\pi_P \left| \frac{1}{N_L} \sum_{X \in \mathcal{X}_L} f(X) - 1 \right| + \left| \frac{1}{N_U} \sum_{X \in \tilde{\mathcal{X}}_U} f(X) - \pi_P \right| \quad (5)$$

Though the PU Loss R_{pu} is biased, Proposition 1 in [62] shows that the original risk can be upper bounded by R_{pu} , so optimizing the upper bound naturally leads to a minimization of the original risk.

Time-Constraint Contrastive Loss. One limitation of the PU Loss function is that it ignores the underlying temporal structure within the data, although the features already contain the temporal dependency. Motivated by Figure 1, we aim to make the loss function handle the information gap between noisy segment-level labels and missing point-level labels. Since the segment is a sequence of time points, the anomaly score should vary smoothly within segments. Therefore, we enforce temporal smoothness between anomaly scores of temporally adjacent points within the same segments by minimizing the difference of scores for adjacent time points as:

$$L_{\text{smooth}} = \frac{1}{N} \sum_{i=1}^N \sum_{j=1}^{T-1} (h(X_i)^j - h(X_i)^{j+1})^2, \quad (6)$$

where $h(\cdot)$ denotes the corresponding anomaly score for each point. Also, we want the anomalous segments to have higher anomaly scores than the normal segments. Thus, we have the separability term:

$$L_{\text{sep}} = \frac{1}{N_U} \sum_{X \in \tilde{\mathcal{X}}_U} f(X) - \frac{1}{N_L} \sum_{X \in \mathcal{X}_L} f(X) \quad (7)$$

By incorporating the smoothness and separability constraints on the segment and point scores, we design a Time-Constraint loss function (TC Loss):

$$L_c = \lambda_1 \cdot L_{\text{smooth}} + \lambda_2 \cdot L_{\text{sep}}, \quad (8)$$

where λ_1 and λ_2 control the strength of L_{smooth} and L_{sep} , respectively. Note that we use batch-wise implementation.

Finally, we present the overall objective of our PU Criterion with PU Loss and time constraint loss, denoted as follows:

$$L = R_{pu} + \lambda \cdot L_c \quad (9)$$

where λ adjusts the importance of L_c .

4.3 Stage-2: Fine-Grained Point Detection

After obtaining the predicted positive segments, we need to further detect the anomalous points. In the data-centric point-level detection module, the points are considered negative in predicted normal segments. For all positive segments, we rank all points according to the anomaly score of each point and then take a user-specified anomaly rate k , where k is a hyperparameter, to get pseudo-predicted labels. For example, when $k=0.5$, the top 50% of the sorted points are regarded as pseudo anomaly points. To get the true anomaly rate in these time points, we put the pseudo prediction result and the feature vector (or simply anomaly scores S) corresponding to each point from the temporal embedding model into the anomaly rate estimator [68] and get the probability of the clean label to automate the threshold selection process. The predicted true anomaly rate is then used to select abnormal time points from all sorted points. In this way, we get the point-level predictions of the time series.

5 Experiments

5.1 Benchmark Datasets

Dataset. For our experiments, we use five temporal datasets collected from various tasks to detect anomalous points. (1) **Electromyography Dataset (EMG)** [30] records 8-channel myographic signals via bracelets worn on subjects' forearms. (2) **Server Machine Dataset7 (SMD)** [43] records the 38 dimensions multivariate time series from Internet server machines over five weeks. (3) **Pooled Server Metrics dataset (PSM)** [1] records 25 dimensions data from multiple eBay server machines. (4) **Mars Science Laboratory (MSL)** [15] records 55 dimensions data from Mars rover. (5) **Soil Moisture Active Passive (SMAP)** [15] records 25 dimensions data and presents the soil samples and telemetry information. The details of the five benchmark datasets are in Table 1.

We split the set of all segments by 7:3 ratio into training and test sets. The average anomalous ratio (AR) of these datasets is 12.22% (point-level). We construct the positive dataset for training by providing only 40% of the anomalous segment-level labels, resulting in a label noise rate of 0.6 (segment-level). The labels for the remaining segments (both anomalous and normal) are not given to construct the unlabeled dataset. We have no access to the point-level labels. Each segment consists of $L = 100$ continuous time points.

Baselines. To evaluate the performance of the proposed method, we compare our approach with 13 different methods. Additionally, we conduct PU learning of point-wise anomalies with noisy point labels as a comparison in Appendix C.1.

- **Unsupervised Learning.** Due to the popularity of utilizing self-supervised methods to detect temporal anomalies, we compare NRdetector with DCdetector [55], Anomaly Transformer [54], and some reconstruction-based methods which compute the point-level anomaly scores from the reconstruction of time series, like AutoFormer [51], FEDformer [63], TimesNet [50], and One-fits-all [64].
- **Semi-supervised learning.** The variants of the unsupervised methods, like AutoFormer++, FEDformer++, TimesNet++, and One-fits-all++, except for Anomaly Transformer and DCdetector. These models are trained by using only normal segments in order to make them utilize given segment-level labels. But note that

the 'normal segments' are actually the unlabeled segments in our setting. Our method is designed in noisy label setting. We aim to compare the noise tolerance of these methods.

- **Weakly supervised learning.** The Multiple Instance Learning (MIL) method, like DeepMIL [44], encourages high anomaly scores at individual time steps based on the segment-level labels. Also, we compare our method with WETAS [22] and TreeMIL [27], which are the main baselines we need to compare.

5.2 Experimental Setting

Evaluation metrics. We adopt various evaluation metrics for comprehensive comparison, including the commonly used F1 score (denoted by $F1$) using both the segment-level ($F1$ -W) and point-level ($F1$ -D) ground truth. Unless otherwise specified, all results are point-level. Note that we do not consider the point adjustment (PA) approach [42, 54, 55] for the evaluation of all methods in the main table. [17] indicates that PA overestimates classifier performance, even though this metric has practical justifications [52]. Thus, we adopt the optimized PA-based metric, PA%K [17], which actually calculates the AUC of PA%K to reduce dependence on the parameter K . Also, we report the recently proposed evaluation measures: affiliation precision/recall pair [14] and Volume under the surface (VUS) [36]. Different metrics provide different views for anomaly evaluations.

Implementation Details. Following the pre-processing methods in [54], we split the dataset into consecutive non-overlapping segments by sliding window. In the implementation phase, running a sliding window in time series data is widely used in TSAD tasks [42] and has little influence on the main design [55]. Thus, we just set the window size L as 100 for all datasets, unlike TreeMIL [27] and WETAS [22]. We use a simple 6 MLP layers as the backbone of the classifier and use ReLU [33] activation between every fully connected layer and Sigmoid activation for the last layer respectively. We use the Adam [18] optimizer with an initial learning rate 0.0001. We set the batch size as 32 and use the batch-size training. In each batch, we identify set of variables on which our loss depends, compute gradient for each variable, and obtain the final gradient through chain rule. The parameters of smoothness and separability constraints in the time constraint loss are set to $\lambda_1 = \lambda_2 = 8 \times 10^{-5}$ for the best performance. The baselines are implemented based on the suggested hyperparameters reported in the corresponding previous literature.

5.3 Performances on Anomaly Detection

We first evaluate our NRdetector with 13 competitive baselines on five real-world multivariate datasets under both pure $F1$ and $F1_{PA\%K}$ metrics as shown in Table 2. It can be seen that our proposed NRdetector achieves the best results under the pure $F1$ score and PA%K $F1$ score on all benchmark datasets. The unsupervised and semi-supervised methods perform considerably worse than the weakly supervised methods in both $F1$ and $F1_{PA\%K}$.

For all unsupervised methods, they cannot achieve as high detection performance as the weakly supervised methods, which indicates the importance of label information. Semi-supervised techniques, which only use the unlabeled segments (know as much label

Table 1: Details of five benchmark datasets. TPS represents the number of the positive segments within the training data. AR (anomaly ratio) represents the abnormal time points proportion of the whole dataset.

Benchmark	Time Points	Source	#Training	#Testing	#TPS	Dimensions	AR (%)
EMG	423825	Myographic Signal Machine	304400	130900	222	8	5.8
SMD	708420	Internet Server Machine	495870	212550	463	38	4.2
PSM	87841	eBay Server Machine	61488	26353	191	25	27.8
MSL	73900	NASA Space Sensors	51610	22119	99	55	10.5
SMAP	427617	NASA Space Sensors	299331	128286	506	25	12.8

Table 2: Performances of NRdetector and other baselines on real-world multivariate datasets. F_1 is the F1-score, $F_{1PA\%K}$ is the optimized PA-based F1 score. The best ones are in Bold, and the second ones are underlined.

Dataset	EMG		SMD		PSM		MSL		SMAP	
	F_1	$F_{1PA\%K}$	F_1	$F_{1PA\%K}$	F_1	$F_{1PA\%K}$	F_1	$F_{1PA\%K}$	F_1	$F_{1PA\%K}$
DCdetector	0.0155	0.0259	0.0105	0.0178	0.0169	0.0272	0.0196	0.0323	0.0169	0.0272
Anomaly Transformer	0.0116	0.0196	0.0181	0.0296	0.0195	0.0334	0.0161	0.0261	0.0173	0.0257
AutoFormer	0.0070	0.0128	0.0646	0.1060	0.0532	0.0821	0.0639	0.1086	0.0091	0.0163
FEDformer	0.0274	0.0484	0.0934	0.1500	0.0494	0.0787	0.0641	0.1090	0.0156	0.0283
TimesNet	0.0089	0.0168	0.0959	0.1373	0.0172	0.0306	0.0731	0.1210	0.0126	0.0216
One-fits-all	0.0388	0.0668	0.0912	0.1381	0.0253	0.0425	0.1234	0.1848	0.0101	0.0172
AutoFormer++	0.0074	0.0134	0.0679	0.1106	0.0855	0.1319	0.0637	0.1082	0.0087	0.0160
FEDformer++	0.0299	0.0527	0.0960	<u>0.1535</u>	0.0892	0.1371	0.0637	0.1083	0.0152	0.0279
TimesNet++	0.0102	0.0186	0.0984	0.1412	0.0342	0.0525	0.0694	0.1154	0.0135	0.0230
One-fits-all++	0.0420	0.0709	0.0884	0.1335	0.0331	0.0535	<u>0.1326</u>	<u>0.1939</u>	0.0139	0.0177
DeepMIL	0.0548	0.0936	0.1009	0.1319	0.2251	0.3279	0.0103	0.0178	0.1024	0.1318
WETAS	<u>0.2446</u>	<u>0.3246</u>	<u>0.1020</u>	0.1171	<u>0.3927</u>	<u>0.4891</u>	0.1113	0.1714	0.1559	0.1775
TreeMIL	0.1696	0.2440	0.0999	0.1164	0.3494	0.4208	0.1258	0.1474	<u>0.2079</u>	<u>0.2397</u>
NRdetector (Ours)	0.4431	0.5174	0.1092	0.1630	0.4990	0.6356	0.2029	0.2219	0.2367	0.2906

Table 3: Multiple metrics results on real-world multivariate datasets. The P and R are the precision and recall. The F_{1PA} is the F1 score using the PA strategy. Aff-P and Aff-R are the precision/recall pair of affiliation metrics. R_{A_R} and R_{A_P} are Range-AUC-ROC and Range-AUC-PR. V_{ROC} and V_{PR} are volumes under the surfaces created based on ROC and PR curves, respectively. The best ones are in Bold.

Methods	F_1	P	R	$F_{1PA\%K}$	F_{1PA}	Aff-P	Aff-R	R_{A_R}	R_{A_P}	V_{ROC}	V_{PR}	
EMG	WETAS	0.2446	0.6334	0.1516	0.3246	0.4612	0.8498	0.2962	0.5483	0.5338	0.5493	0.5291
	TreeMIL	0.1696	0.5689	0.0997	0.2440	0.5688	0.7829	0.4956	0.5863	0.5825	0.5851	0.5764
	NRdetector	0.4431	0.5660	0.3640	0.5174	0.6188	0.8916	0.5705	0.6579	0.5894	0.6556	0.5808
SMD	WETAS	0.1020	0.0762	0.1542	0.1171	0.1370	0.5259	0.6530	0.5120	0.1602	0.5115	0.1581
	TreeMIL	0.0999	0.0612	0.2723	0.1164	0.1601	0.5212	0.7880	0.5510	0.2334	0.5477	0.2300
	NRdetector	0.1092	0.2232	0.0722	0.1630	0.6761	0.6363	0.5317	0.6108	0.5029	0.6118	0.5041
PSM	WETAS	0.3927	0.4651	0.3398	0.4891	0.6532	0.6145	0.6550	0.7128	0.7681	0.7055	0.7549
	TreeMIL	0.3494	0.4103	0.3043	0.4208	0.6686	0.6756	0.7036	0.7273	0.7799	0.7367	0.7766
	NRdetector	0.4990	0.6976	0.3884	0.6356	0.8856	0.7491	0.5374	0.7462	0.7982	0.7261	0.7837

information as our method) as the training data, marginally outperform unsupervised methods but still lag behind weakly supervised ones. The presence of anomalous segments within unlabeled data highlights a limitation of semi-supervised methods—they struggle to effectively handle noise within ‘normal’ (actually unlabeled) data. This shed light on the importance of how to utilize the positive segment-level labels and tackle the noise in the label information, as these factors significantly influence the final detection performance.

As the recent weakly supervised methods WETAS and TreeMIL achieve better results than other baseline models, we mainly compare NRdetector with them under different evaluation metrics as shown in Table 3. We can learn from the results that our method performs better than WETAS and TreeMIL in most metrics. Our proposed approach can effectively handle noise, making our method more robust to segment-level label noise, while WETAS and TreeMIL rely more on accurate label information, especially the normal label.

From Table 2 and Table 4, We can see our method achieves robust results under different label noise rates. While the other methods are

Table 4: Performances of NRdetector and weakly supervised learning baselines on real-world multivariate datasets under different label noise rates. Label noise Rate is the proportion of positive segments seen as unlabeled, $e_1 := P(\check{Y} = 0|Y = 1)$. F1 is the F1-score, $F1_{PA\%K}$ is the optimized PA-based F1 score. The best ones are in Bold, and the second ones are underlined.

Label Noise Rate	Dataset	EMG		SMD		PSM		MSL		SMAP	
	Methods	F1	$F1_{PA\%K}$	F1	$F1_{PA\%K}$	F1	$F1_{PA\%K}$	F1	$F1_{PA\%K}$	F1	$F1_{PA\%K}$
0.4	DeepMIL	0.0484	0.0821	0.0865	0.1203	0.2274	0.3374	0.0225	0.0398	0.1391	0.1898
	WETAS	<u>0.3906</u>	<u>0.4929</u>	0.1393	<u>0.1603</u>	0.2978	0.3884	0.0753	0.1186	<u>0.1506</u>	<u>0.2002</u>
	TreeMIL	0.2561	0.3437	0.1247	0.1556	<u>0.4665</u>	<u>0.5379</u>	<u>0.1257</u>	<u>0.1494</u>	0.1220	0.1294
	NRdetector	0.5599	0.6212	<u>0.1280</u>	0.1823	0.5548	0.6883	0.1395	0.1531	0.1957	0.2012
0.2	DeepMIL	0.0924	0.1511	0.1026	0.1306	0.1654	0.2564	0.0145	0.0247	0.0686	0.1149
	WETAS	<u>0.5543</u>	<u>0.6530</u>	<u>0.1297</u>	<u>0.1671</u>	0.2110	0.3172	0.0987	0.1509	0.0971	0.1560
	TreeMIL	0.5284	0.6010	0.1279	0.1510	<u>0.3812</u>	<u>0.4367</u>	<u>0.1126</u>	<u>0.1637</u>	<u>0.1715</u>	0.2017
	NRdetector	0.6057	0.6638	0.1313	0.1810	0.5202	0.5301	0.1745	0.1829	0.1879	<u>0.1965</u>
0.0	DeepMIL	0.0901	0.1446	0.0636	0.0942	0.4276	0.5421	0.0022	0.0039	0.1033	0.1324
	WETAS	0.6405	0.7403	<u>0.1308</u>	<u>0.1715</u>	0.4879	0.5621	0.1089	0.1608	0.1381	0.1496
	TreeMIL	0.5443	0.6040	0.1769	0.2161	0.5759	0.6229	0.1221	<u>0.1596</u>	<u>0.1508</u>	0.1956
	NRdetector	<u>0.6141</u>	<u>0.7207</u>	0.1255	0.1687	<u>0.5130</u>	<u>0.5905</u>	<u>0.1144</u>	0.1246	0.1704	<u>0.1856</u>

less tolerant of noisy label and show unstable performance under the high label noise rate. The results demonstrate the limitations of current unsupervised methods, especially when the anomalies lie in the training data for building the normal patterns. When there is less noise in the label, NRdetector still outperforms WETAS and TreeMIL, but the gap is not very large. For example, when the label noise rate is 0.2, the F1 scores on the EMG dataset only decrease by 0.051 and 0.077, respectively. However, in the label noise rate of 0.6 cases, the NRdetector completely outperforms the three methods by at least 0.2 on the EMG dataset. When the label noise rate is 0.0, turning the problem into a MIL problem, our method achieved the second-best performance on most datasets, comparable to WETAS and TreeMIL.

5.4 Ablation Studies

To better understand how each component in NRdetector contributes to the final accurate anomaly detection, we conduct extensive ablation studies.

Model Structure. In the temporal embedding module, WETAS is adopted as a representation framework to get the informative temporal features. We conduct an ablation study on how the representation model structure (both Di-CNN and Transformer [46] are seven layers) affects the performance of our method in Table 8 in the Appendix. The results indicate that Di-CNN and Transformer architectures have basically the same performance, but the former performs slightly better in multiple metrics.

Sample Selector. With confidence-based sample selection modules, we can see that NRdetector gains the best performance from Table 5. Both confidence-based extraction and label propagation processes will degrade the performance of our model when used individually. However, if they are utilized simultaneously, the performance improves. This may be because only reliable extraction loses most of the data information, while using only label propagation may lead to more pseudo-positive segments in the similarity-based network.

PU Criterion. Table 6 shows the ablation study of PU Criterion. According to the loss function definition in Section 4.2.3, we use

PU Loss, denoted as R_{pu} , and TC Loss, denoted as L_{tc} . To utilize the provided segment-level labels, we use the binary cross entropy as the basic loss function. We can find that our PU Criterion leads to a great improvement from those without PU Loss. Also, the results demonstrate the effectiveness of the proposed time constraint loss.

We find that HOC [68] can automate the threshold selection process, which improves the performance of point-level detection. These ablation studies demonstrate the effectiveness of our approach.

5.5 Additional Analysis

We aim to study the flexibility provided by our method, which utilizes only partial segment-level labels, and compare its detection performance with that of point-level PU learning methods and augmentation-based methods (see Appendix C.1).

Point-level PU learning. We use the same temporal embedding as our method to represent the temporal feature of each time series point for a fair comparison, as these methods [19, 62] are not specifically designed for time series data. In terms of input data, these methods require point-level positive data and unlabeled data. For all labeled anomaly segments in our setting (segment-level label noise rate = 0.6), the anomaly points within these segments constitute the positive dataset, while the normal points within these segments and points in other segments (both actual anomaly segments and normal segments) constitute the unlabeled dataset. This ensures that the label information known to the point-level PU method is as close as possible to ours, avoiding the situation where knowing too many labels renders the comparison meaningless.

Since NCAD [4] is not the most recent SOTA unsupervised learning method, we use the provided supervised setting. However, because point-level labels are required, we provide point-level labels based on the segment-level label noise rate of 0.6 (as mentioned above). Note that this kind of labeling actually contains more information than segment-level labeling.

The results, shown in Table 7, indicate that our approach performs better than point-level PU learning methods while providing

Table 5: Ablation Studies on Sample Selector in NRdetector . 'Extraction' is the process of obtaining reliable negatives (RN) based on the confidence, and 'Propagation' is the process of propagating the label to the neighboring nodes. F1-W denotes the F1 score between the actual segment-level labels and the segment-level predictions. F1-D denotes the F1 score between dense labels and the point-level predictions. F1-D (w/o HOC) denotes the F1 score with random noise rate k. The best ones are in Bold.

Sample Selector		EMG			PSM			SMAP		
Extraction	Propagation	F1-W	F1-D(w/o HOC)	F1-D	F1-W	F1-D(w/o HOC)	F1-D	F1-W	F1-D(w/o HOC)	F1-D
✗	✗	0.4643	0.3619	0.4130	0.4875	0.3446	0.4916	0.2256	0.0917	0.1878
✓	✗	0.4294	0.3485	0.4055	0.4731	0.4382	0.4501	0.1417	0.0516	0.1318
✗	✓	0.4125	0.3124	0.4084	0.4792	0.4574	0.4676	0.2418	0.0752	0.2009
✓	✓	0.4824	0.3800	0.4431	0.4920	0.4566	0.4990	0.2449	0.2097	0.2367

Table 6: Ablation Studies on PU Criterion in NRdetector . F1-W denotes the F1 score between actual segment-level labels and the segment-level predictions. F1-D denotes the F1 score between dense labels and the point-level predictions. F1-D (w/o HOC) denotes the F1 score with random noise rate k. The best ones are in Bold.

PU Criterion			EMG			PSM			SMAP		
L_{bce}	R_{pu}	L_{tc}	F1-W	F1-D(w/o HOC)	F1-D	F1-W	F1-D(w/o HOC)	F1-D	F1-W	F1-D(w/o HOC)	F1-D
✓	✗	✗	0.3871	0.3110	0.3695	0.4712	0.3159	0.4811	0.2192	0.1772	0.1794
✓	✗	✓	0.4294	0.3485	0.4055	0.4792	0.3674	0.4648	0.2071	0.0793	0.1713
✗	✓	✗	0.4734	0.3751	0.4406	0.4876	0.3446	0.4802	0.1743	0.0971	0.1534
✗	✓	✓	0.4824	0.3800	0.4431	0.4920	0.4566	0.4990	0.2449	0.2097	0.2367

Table 7: Performances of NRdetector and point-level PU learning method on real-world multivariate datasets when the segment-level label noise rate is 0.6. F1 is the F1-score, $F1_{PA\%K}$ is the optimized PA-based F1 score. The best ones are in Bold.

Dataset	EMG		SMD		PSM		MSL		SMAP	
	F1	$F1_{PA\%K}$	F1	$F1_{PA\%K}$	F1	$F1_{PA\%K}$	F1	$F1_{PA\%K}$	F1	$F1_{PA\%K}$
Point-level nnPU [19]	0.1077	0.1077	0.0735	0.0735	0.4538	0.4538	0.0775	0.0775	0.1293	0.1293
Point-level Dist-PU [62]	0.2944	0.3726	0.0735	0.0735	0.4451	0.5799	0.0983	0.1498	0.1223	0.1743
Point-level NCAD [4]	0.0651	0.1563	0.0676	0.9318	0.0159	0.0182	0.0414	0.0987	0.0217	0.0254
Segment-level NRdetector (Ours)	0.4431	0.5174	0.1092	0.1630	0.4990	0.6356	0.2029	0.2219	0.2367	0.2906

greater flexibility by utilizing only segment-level labels. It also outperforms NCAD using noisy point-level labels.

5.6 Hyperparameter Studies

To evaluate the robustness of our framework under different hyper-parameters, we vary the parameters to investigate how the model performance varies. Figure 3(a) shows the performance on the MSL dataset under different Class Prior. The result demonstrates that NRdetector is robust with a wide range of class prior, alleviating the need for PU Loss to estimate class prior accurately. Figure 3(b) shows the performance under different batch sizes. It indicates that NRdetector achieves the best performance with the batch size 32. More experimental results are left in Appendix C.

6 Conclusion

We have proposed NRdetector, a noise-resilient multivariate TSAD framework with a novel contrastive-based loss function to bridge the gap between noisy segment labels and missing point labels. We have experimentally demonstrated the effectiveness of each component in our framework. Comparisons with state-of-the-art baselines on several real-world time series benchmarks reveal that NRdetector consistently outperforms existing time series anomaly detection methods in the noisy label setting. Future directions involve exploring the power of large language models (LLMs) on

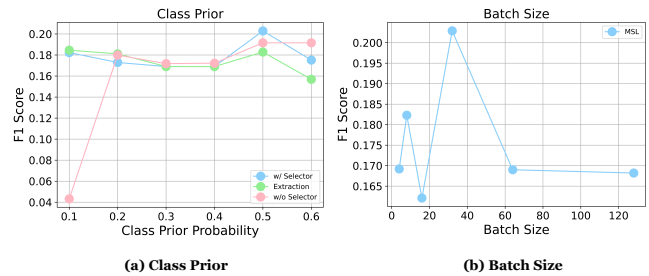


Figure 3: Parameter sensitivity studies of hyper-parameters, Class Prior and Batch Size in NRdetector. Both studies are conducted on the MSL dataset.

such tasks and implementing this approach in real-world label noise scenarios.

References

- [1] Ahmed Abdulaal, Zhuanghua Liu, and Tomer Lancewicki. 2021. Practical approach to asynchronous multivariate time series anomaly detection and localization. In *Proceedings of the 27th ACM SIGKDD conference on knowledge discovery & data mining*. 2485–2494.
- [2] Peter L Bartlett, Michael I Jordan, and Jon D McAuliffe. 2006. Convexity, classification, and risk bounds. *J. Amer. Statist. Assoc.* 101, 473 (2006), 138–156.
- [3] Jessa Bekker and Jesse Davis. 2020. Learning from positive and unlabeled data: A survey. *Machine Learning* 109 (2020), 719–760.
- [4] Chris U Carmona, François-Xavier Aubet, Valentin Flunkert, and Jan Gasthaus. 2021. Neural contextual anomaly detection for time series. *arXiv preprint arXiv:2107.07702* (2021).
- [5] Feiyi Chen, Zhen Qing, Yingying Zhang, Shuiguang Deng, Yi Xiao, Guansong Pang, and Qingsong Wen. 2023. LARA: A Light and Anti-overfitting Retraining Approach for Unsupervised Anomaly Detection. *arXiv preprint arXiv:2310.05668* (2023).
- [6] Xuxi Chen, Wuyang Chen, Tianlong Chen, Ye Yuan, Chen Gong, Kewei Chen, and Zhangyang Wang. 2020. Self-pu: Self boosted and calibrated positive-unlabeled training. In *International Conference on Machine Learning*. PMLR, 1510–1519.
- [7] Zahra Zamanzadeh Darban, Geoffrey I Webb, Shirui Pan, Charu C Aggarwal, and Mahsa Salehi. 2025. CARLA: Self-supervised contrastive representation learning for time series anomaly detection. *Pattern Recognition* 157 (2025), 110874.
- [8] Mariana Caravanti de Souza, Bruno Magalhães Nogueira, Rafael Geraldeli Rossi, Ricardo Marcondes Marcacini, Bruce Neves Dos Santos, and Solange Oliveira Rezende. 2022. A network-based positive and unlabeled learning approach for fake news detection. *Machine Learning* 111, 10 (2022), 3549–3592.
- [9] Marthinus C Du Plessis, Gang Niu, and Masashi Sugiyama. 2014. Analysis of learning from positive and unlabeled data. *Advances in neural information processing systems* 27 (2014).
- [10] Eman Abd Elaziz, Radwa Fathalla, and Mohamed Shaheen. 2023. Deep reinforcement learning for data-efficient weakly supervised business process anomaly detection. *Journal of Big Data* 10, 1 (2023), 33.
- [11] Jingkun Gao, Xiaomin Song, Qingsong Wen, Pichao Wang, Liang Sun, and Huan Xu. 2020. RobustTAD: Robust time series anomaly detection via decomposition and convolutional neural networks. *arXiv preprint arXiv:2002.09545* (2020).
- [12] Bo Han, Quanming Yao, Xingrui Yu, Gang Niu, Miao Xu, Weihua Hu, Ivor Tsang, and Masashi Sugiyama. 2018. Co-teaching: Robust training of deep neural networks with extremely noisy labels. *Advances in neural information processing systems* 31 (2018).
- [13] Wenpeng Hu, Ran Le, Bing Liu, Feng Ji, Jinwen Ma, Dongyan Zhao, and Rui Yan. 2021. Predictive adversarial learning from positive and unlabeled data. In *Proceedings of the AAAI conference on artificial intelligence*, Vol. 35. 7806–7814.
- [14] Alexis Huet, Jose Manuel Navarro, and Dario Rossi. 2022. Local evaluation of time series anomaly detection algorithms. In *Proceedings of the 28th ACM SIGKDD Conference on Knowledge Discovery and Data Mining*. 635–645.
- [15] Kyle Hundman, Valentino Constantinou, Christopher Laporte, Ian Colwell, and Tom Soderstrom. 2018. Detecting spacecraft anomalies using lstms and nonparametric dynamic thresholding. In *Proceedings of the 24th ACM SIGKDD international conference on knowledge discovery & data mining*. 387–395.
- [16] Dongmin Kim, Sunghyun Park, and Jaegul Choo. 2023. When Model Meets New Normals: Test-time Adaptation for Unsupervised Time-series Anomaly Detection. *arXiv preprint arXiv:2312.11976* (2023).
- [17] Siwon Kim, Kukjin Choi, Hyun-Soo Choi, Byunghan Lee, and Sungroh Yoon. 2022. Towards a rigorous evaluation of time-series anomaly detection. In *Proceedings of the AAAI Conference on Artificial Intelligence*, Vol. 36. 7194–7201.
- [18] Diederik P Kingma and Jimmy Ba. 2014. Adam: A method for stochastic optimization. *arXiv preprint arXiv:1412.6980* (2014).
- [19] Ryuichi Kiryo, Gang Niu, Marthinus C Du Plessis, and Masashi Sugiyama. 2017. Positive-unlabeled learning with non-negative risk estimator. *Advances in neural information processing systems* 30 (2017).
- [20] Chih-Yu Andrew Lai, Fan-Keng Sun, Zhengqi Gao, Jeffrey H Lang, and Duane Boning. 2024. Nominality score conditioned time series anomaly detection by point/sequential reconstruction. *Advances in Neural Information Processing Systems* 36 (2024).
- [21] Kwei-Herng Lai, Daochen Zha, Junjie Xu, Yue Zhao, Guanchu Wang, and Xia Hu. 2021. Revisiting time series outlier detection: Definitions and benchmarks. In *Thirty-fifth conference on neural information processing systems datasets and benchmarks track (round 1)*.
- [22] Dongha Lee, Sehun Yu, Hyunjun Ju, and Hwanjo Yu. 2021. Weakly supervised temporal anomaly segmentation with dynamic time warping. In *Proceedings of the IEEE/CVF International Conference on Computer Vision*. 7355–7364.
- [23] Longyuan Li, Junchi Yan, Qingsong Wen, Yaohui Jin, and Xiaokang Yang. 2022. Learning robust deep state space for unsupervised anomaly detection in contaminated time-series. *IEEE Transactions on Knowledge and Data Engineering* (2022).
- [24] Xiaoli Li and Bing Liu. 2003. Learning to classify texts using positive and unlabeled data. In *IJCAI*, Vol. 3. 587–592.
- [25] Min Lin, Qiang Chen, and Shuicheng Yan. 2013. Network in network. *arXiv preprint arXiv:1312.4400* (2013).
- [26] Bing Liu, Wee Sun Lee, Philip S Yu, and Xiaoli Li. 2002. Partially supervised classification of text documents. In *ICML*, Vol. 2. Sydney, NSW, 387–394.
- [27] Chen Liu, Shibo He, Haoyu Liu, and Shizhong Li. 2024. TreeMIL: A Multi-instance Learning Framework for Time Series Anomaly Detection with Inexact Supervision. *arXiv preprint arXiv:2401.11235* (2024).
- [28] Tongliang Liu and Dacheng Tao. 2015. Classification with noisy labels by importance reweighting. *IEEE Transactions on pattern analysis and machine intelligence* 38, 3 (2015), 447–461.
- [29] Yang Liu and Hongyi Guo. 2020. Peer loss functions: Learning from noisy labels without knowing noise rates. In *International conference on machine learning*. PMLR, 6226–6236.
- [30] Sergey Lobov, Nadia Krilova, Innokentiy Kastalskiy, Victor Kazantsev, and Valeri A Makarov. 2018. Latent factors limiting the performance of sEMG-interfaces. *Sensors* 18, 4 (2018), 1122.
- [31] Chuan Luo, Pu Zhao, Chen Chen, Bo Qiao, Chao Du, Hongyu Zhang, Wei Wu, Shaowei Cai, Bing He, Saravanakumar Rajmohan, et al. 2021. Pulns: Positive-unlabeled learning with effective negative sample selector. In *Proceedings of the AAAI Conference on Artificial Intelligence*, Vol. 35. 8784–8792.
- [32] Shuangxun Ma and Ruisheng Zhang. 2017. PU-IP: A novel approach for positive and unlabeled learning by label propagation. In *2017 IEEE International Conference on Multimedia & Expo Workshops (ICMEW)*. IEEE, 537–542.
- [33] Vinod Nair and Geoffrey E Hinton. 2010. Rectified linear units improve restricted boltzmann machines. In *Proceedings of the 27th international conference on machine learning (ICML-10)*. 807–814.
- [34] Minh Nhut Nguyen, Xiao-Li Li, and See-Kiong Ng. 2011. Positive unlabeled learning for time series classification. In *Twenty-Second International Joint Conference on Artificial Intelligence*. Citeseer.
- [35] Aaron van den Oord, Sander Dieleman, Heiga Zen, Karen Simonyan, Oriol Vinyals, Alex Graves, Nal Kalchbrenner, Andrew Senior, and Koray Kavukcuoglu. 2016. Wavenet: A generative model for raw audio. *arXiv preprint arXiv:1609.03499* (2016).
- [36] John Paparrizos, Paul Boniol, Themis Palpanas, Ruy S Tsay, Aaron Elmore, and Michael J Franklin. 2022. Volume under the surface: a new accuracy evaluation measure for time-series anomaly detection. *Proceedings of the VLDB Endowment* 15, 11 (2022), 2774–2787.
- [37] Daehyung Park, Yuuna Hoshi, and Charles C Kemp. 2018. A multimodal anomaly detector for robot-assisted feeding using an lstm-based variational autoencoder. *IEEE Robotics and Automation Letters* 3, 3 (2018), 1544–1551.
- [38] Giorgio Patrini, Alessandro Rozza, Aditya Krishna Menon, Richard Nock, and Lizhen Qu. 2017. Making deep neural networks robust to label noise: A loss correction approach. In *Proceedings of the IEEE conference on computer vision and pattern recognition*. 1944–1952.
- [39] Lorenzo Perini, Vincent Vercauteren, and Jesse Davis. 2023. Learning from Positive and Unlabeled Multi-Instance Bags in Anomaly Detection. In *Proceedings of the 29th ACM SIGKDD Conference on Knowledge Discovery and Data Mining*. 1897–1906.
- [40] Lukas Ruff, Robert Vandermeulen, Nico Goernitz, Lucas Deecke, Shoaib Ahmed Siddiqui, Alexander Binder, Emmanuel Müller, and Marius Kloft. 2018. Deep one-class classification. In *International conference on machine learning*. PMLR, 4393–4402.
- [41] Artem Ryzhikov, Maxim Borisyak, Andrey Ustyuzhanin, and Denis Derkach. 2021. NEAD: fixing anomaly detection using normalizing flows. *PeerJ Computer Science* 7 (2021), e757.
- [42] Lifeng Shen, Zhuocong Li, and James Kwok. 2020. Timeseries anomaly detection using temporal hierarchical one-class network. *Advances in Neural Information Processing Systems* 33 (2020), 13016–13026.
- [43] Ya Su, Youjian Zhao, Chenhao Niu, Rong Liu, Wei Sun, and Dan Pei. 2019. Robust anomaly detection for multivariate time series through stochastic recurrent neural network. In *Proceedings of the 25th ACM SIGKDD international conference on knowledge discovery & data mining*. 2828–2837.
- [44] Waqas Sultani, Chen Chen, and Mubarak Shah. 2018. Real-world anomaly detection in surveillance videos. In *Proceedings of the IEEE conference on computer vision and pattern recognition*. 6479–6488.
- [45] Yuting Sun, Guansong Pang, Guanhua Ye, Tong Chen, Xia Hu, and Hongzhi Yin. 2023. Unraveling the Anomaly in Time Series Anomaly Detection: A Self-supervised Tri-domain Solution. *arXiv preprint arXiv:2311.11235* (2023).
- [46] Ashish Vaswani, Noam Shazeer, Niki Parmar, Jakob Uszkoreit, Llion Jones, Aidan N Gomez, Łukasz Kaiser, and Illia Polosukhin. 2017. Attention is all you need. *Advances in neural information processing systems* 30 (2017).
- [47] Rui Wang, Xudong Mou, Renyu Yang, Kai Gao, Pin Liu, Chongwei Liu, Tianyu Wo, and Xudong Liu. 2024. CutAddPaste: Time Series Anomaly Detection by Exploiting Abnormal Knowledge. In *Proceedings of the 30th ACM SIGKDD Conference on Knowledge Discovery and Data Mining*. 3176–3187.
- [48] Jiaheng Wei, Hangyu Liu, Tongliang Liu, Gang Niu, Masashi Sugiyama, and Yang Liu. 2021. To smooth or not? when label smoothing meets noisy labels. *arXiv preprint arXiv:2106.04149* (2021).

- [49] Jiaheng Wei, Zhaowei Zhu, Hao Cheng, Tongliang Liu, Gang Niu, and Yang Liu. 2021. Learning with noisy labels revisited: A study using real-world human annotations. *arXiv preprint arXiv:2110.12088* (2021).
- [50] Haixu Wu, Tengge Hu, Yong Liu, Hang Zhou, Jianmin Wang, and Mingsheng Long. 2022. Timesnet: Temporal 2d-variation modeling for general time series analysis. *arXiv preprint arXiv:2210.02186* (2022).
- [51] Haixu Wu, Jiehui Xu, Jianmin Wang, and Mingsheng Long. 2021. Autoformer: Decomposition transformers with auto-correlation for long-term series forecasting. *Advances in Neural Information Processing Systems* 34 (2021), 22419–22430.
- [52] Haowen Xu, Wenxiao Chen, Nengwen Zhao, Zeyan Li, Jiahao Bu, Zhihan Li, Ying Liu, Youjian Zhao, Dan Pei, Yang Feng, et al. 2018. Unsupervised anomaly detection via variational auto-encoder for seasonal kpis in web applications. In *Proceedings of the 2018 world wide web conference*. 187–196.
- [53] Hongzuo Xu, Yijie Wang, Songlei Jian, Qing Liao, Yongjun Wang, and Guansong Pang. 2024. Calibrated one-class classification for unsupervised time series anomaly detection. *IEEE Transactions on Knowledge and Data Engineering* (2024).
- [54] Jiehui Xu, Haixu Wu, Jianmin Wang, and Mingsheng Long. 2021. Anomaly transformer: Time series anomaly detection with association discrepancy. *arXiv preprint arXiv:2110.02642* (2021).
- [55] Yiyuan Yang, Chaoli Zhang, Tian Zhou, Qingsong Wen, and Liang Sun. 2023. DCdetector: Dual Attention Contrastive Representation Learning for Time Series Anomaly Detection. In *Proceedings of the 28th ACM SIGKDD Conference on Knowledge Discovery and Data Mining*.
- [56] Chen Zhang, Guorong Li, Yuankai Qi, Shuhui Wang, Laiyun Qing, Qingming Huang, and Ming-Hsuan Yang. 2023. Exploiting Completeness and Uncertainty of Pseudo Labels for Weakly Supervised Video Anomaly Detection. In *Proceedings of the IEEE/CVF Conference on Computer Vision and Pattern Recognition*. 16271–16280.
- [57] Chaoli Zhang, Tian Zhou, Qingsong Wen, and Liang Sun. 2022. TFAD: A decomposition time series anomaly detection architecture with time-frequency analysis. In *Proceedings of the 31st ACM International Conference on Information & Knowledge Management*. 2497–2507.
- [58] Jiaqi Zhang, Zhenzhen Wang, Junsong Yuan, and Yap-Peng Tan. 2017. Positive and unlabeled learning for anomaly detection with multi-features. In *Proceedings of the 25th ACM international conference on Multimedia*. 854–862.
- [59] Kexin Zhang, Qingsong Wen, Chaoli Zhang, Liang Sun, and Yong Liu. 2022. Time Series Anomaly Detection using Skip-Step Contrastive Predictive Coding. In *NeurIPS 2022 Workshop: Self-Supervised Learning-Theory and Practice*.
- [60] Shenglin Zhang, Chenyu Zhao, Yicheng Sui, Ya Su, Yongqian Sun, Yuzhi Zhang, Dan Pei, and Yizhe Wang. 2021. Robust KPI anomaly detection for large-scale software services with partial labels. In *2021 IEEE 32nd International Symposium on Software Reliability Engineering (ISSRE)*. IEEE, 103–114.
- [61] Yingying Zhang, Zhengxiong Guan, Huajie Qian, Leili Xu, Hengbo Liu, Qingsong Wen, Liang Sun, Junwei Jiang, Lunting Fan, and Min Ke. 2021. CloudRCA: A root cause analysis framework for cloud computing platforms. In *Proceedings of the 30th ACM International Conference on Information & Knowledge Management*. 4373–4382.
- [62] Yunrui Zhao, Qianqian Xu, Yangbangyan Jiang, Peisong Wen, and Qingming Huang. 2022. Dist-pu: Positive-unlabeled learning from a label distribution perspective. In *Proceedings of the IEEE/CVF Conference on Computer Vision and Pattern Recognition*. 14461–14470.
- [63] Tian Zhou, Ziqing Ma, Qingsong Wen, Xue Wang, Liang Sun, and Rong Jin. 2022. Fedformer: Frequency enhanced decomposed transformer for long-term series forecasting. In *International Conference on Machine Learning*. PMLR, 27268–27286.
- [64] Tian Zhou, Peisong Niu, Xue Wang, Liang Sun, and Rong Jin. 2023. One Fits All: Power General Time Series Analysis by Pretrained LM. *arXiv preprint arXiv:2302.11939* (2023).
- [65] Zhi-Hua Zhou. 2004. Multi-instance learning: A survey. *Department of Computer Science & Technology, Nanjing University, Tech. Rep* 1 (2004).
- [66] Zhaowei Zhu, Tongliang Liu, and Yang Liu. 2021. A second-order approach to learning with instance-dependent label noise. In *Proceedings of the IEEE/CVF conference on computer vision and pattern recognition*. 10113–10123.
- [67] Zhaowei Zhu, Tianyi Luo, and Yang Liu. 2021. The rich get richer: Disparate impact of semi-supervised learning. *arXiv preprint arXiv:2110.06282* (2021).
- [68] Zhaowei Zhu, Yiwen Song, and Yang Liu. 2021. Clusterability as an alternative to anchor points when learning with noisy labels. In *International Conference on Machine Learning*. PMLR, 12912–12923.
- [69] Zhaowei Zhu, Jialu Wang, Hao Cheng, and Yang Liu. 2023. Unmasking and improving data credibility: A study with datasets for training harmless language models. *arXiv preprint arXiv:2311.11202* (2023).
- [70] Zhangchi Zhu, Lu Wang, Pu Zhao, Chao Du, Wei Zhang, Hang Dong, Bo Qiao, Qingwei Lin, Saravan Rajmohan, and Dongmei Zhang. 2023. Robust Positive-Unlabeled Learning via Noise Negative Sample Self-correction. In *Proceedings of the 29th ACM SIGKDD Conference on Knowledge Discovery and Data Mining*. 3663–3673.

A Algorithms

Algorithm 1: Sample Selector: Confidence-based Extraction

Input :

- \mathcal{X}_L , a set of labeled positive segments
- \mathcal{X}_U , a set of unlabeled segments
- m , number of iterations
- λ_0 , controls the size of set to be filtered out
- W , similarity matrix calculated by Katz index

Output:

- \mathcal{X}_{RN} , set of extracted reliable positive segments

- 1 initialize the \mathcal{X}_{RN} and \mathcal{X}_{out} set;
 - 2 initialize $k = 0$;
 - 3 **repeat**
 - 4 based on W , calculate S_{X_i} , $S_{X_i} = \frac{\sum_{j=1}^{N_p} W_{i,j}}{N_p}$; // S_{X_i} is the mean similarity between an unlabeled segment X_i and all labeled positive segments;
 - 5 rank each segment X_i according to the S_{X_i} , $X_i \in \mathcal{X}_U$;
 - 6 $out' \leftarrow$ the top $\frac{\lambda_0}{m} \times N_p$ ranked examples in \mathcal{X}_U ;
 - 7 $\mathcal{X}_{out} \leftarrow \mathcal{X}_{out} \cup \mathcal{X}_{out'}$, $\mathcal{X}_U \leftarrow \mathcal{X}_U - \mathcal{X}_{out'}$;
 - 8 $k = k + 1$;
 - 9 **until** $k = m$;
 - 10 based on W , calculate S_{X_i} , $X_i \in \mathcal{X}_U - \mathcal{X}_{out}$,
 - 11 $S_{X_i} = \frac{\sum_{j=1}^{N_p+|out|} W_{i,j}}{N_p+|out|}$;
 - 12 rank each segment X_i according to the S_{X_i} ,
 - 13 $X_i \in \mathcal{X}_U - \mathcal{X}_{out}$;
 - 14 $\mathcal{X}_{RN} \leftarrow$ the bottom $N_p + |\mathcal{X}_{out}|$ ranked examples in $\mathcal{X}_U - \mathcal{X}_{out}$;
 - 15 **return** \mathcal{X}_{RN}
-

Algorithm 2: Sample Selector: Label Propagation

Input :

- X , a set of all segments
- F_X , the label information //For $X_i \in \mathcal{X}_p$, the label is $[0,1]$; for $X_i \in \mathcal{X}_{RN}$, the label is $[1,0]$; the label of other segments are $[0,0]$
- w , connection weights between nodes

Output:

- $F_{\mathcal{X}_U}$, class information for unlabeled segments

- 1 $D \leftarrow \text{diag}(w \cdot I_N)$; // $\text{diag}(\dots)$ is the matrix diagonal operator;
 - 2 $P \leftarrow (D^{-1}) \cdot w$;
 - 3 **while** there is no convergence or maximum number of iterations not being reached **do**
 - 4 $F_X \leftarrow P \cdot F_X$;
 - 5 $F_{\mathcal{X}_L} \leftarrow Y_{\mathcal{X}_L}$;
 - 6 **end while**
 - 7 **return** $F_{\mathcal{X}_U}$
-

Table 8: Ablation Studies on model structure for temporal embedding module in NRdetector. F1-W denotes the F1 score between the actual segment-level labels and the segment-level predictions. F1-D denotes the F1 score between dense labels and the point-level predictions. F1-D (w/o HOC) denotes the F1 score with random anomaly rate k. The best ones are in Bold.

Dataset	EMG			PSM			SMAP		
	F1-W	F1-D(w/o HOC)	F1-D	F1-W	F1-D(w/o HOC)	F1-D	F1-W	F1-D(w/o HOC)	F1-D
Di-CNN	0.4824	0.3800	0.4431	0.4780	0.3647	0.4990	0.2449	0.2097	0.2367
Transformer	0.4734	0.3751	0.4406	0.5301	0.3444	0.4930	0.2410	0.2051	0.2354

Table 9: Experimental results comparing our method with CARLA and CutAddPaste on the EMG, SMD, and PSM datasets under a 0.6 label noise rate. F1-W denotes the F1 score between the actual segment-level labels and the segment-level predictions.

Method	EMG			SMD			PSM		
	F1-W	F1	F1 _{PA%K}	F1-W	F1	F1 _{PA%K}	F1-W	F1	F1 _{PA%K}
CARLA [7]	0.1918	0.0939	0.1044	0.1383	0.0642	0.0793	0.5589	0.1882	0.1882
CutAddPaste(floating) [47]	0.4153	0.1869	0.2362	0.1754	0.0699	0.0844	0.5589	0.1882	0.1882
NRdetector (Ours)	0.4824	0.4431	0.5174	0.1693	0.1092	0.1630	0.4780	0.4990	0.6356

Table 10: The values of hyperparameters used in NRdetector

	EMG	SMD	PSM	MSL	SMAP
<i>prior</i>	0.25	0.8	0.4	0.5	0.5
<i>anoamly_ratio</i>	0.65	0.15	0.6	0.8	0.9

B Proof for Theorems

B.1 Upper Bound

We consider the case where $Y|X$ is confident, i.e., each feature X belongs to one particular true class Y with probability 1, which is generally held in classification problems [28]. Due to the specificity of the PU setting, where e_0 equals 0, we could get the following theorem based on Lemma 2 and Theorem 2 in [67].

THEOREM B.1. *With probability at least $1 - \delta$, the generalization error on datasets \tilde{D} is upper-bounded by*

$$R_{\mathcal{D}}(\hat{f}) \leq \bar{\eta} + \sqrt{\frac{2 \log\left(\frac{4}{\delta}\right)}{N}} + P(\tilde{Y} \neq \tilde{Y}^*),$$

where $\bar{\eta}$ is the expected label error in the pseudo noisy dataset \tilde{D} .

LEMMA B.2. *For any feature X , if $Y|X$ is confident, $\eta(X)$ is the error rate of the model prediction on X , i.e., $\exists i \in [K] : P(Y = i|X) = 1 \Rightarrow \eta(X) = P(\tilde{Y} \neq Y|X) = e(X)$.*

Based on Lemma B.2, for PU setting, we have $\eta(X) = P(\tilde{Y} \neq Y|X) = e(X)$. In PU setting, $e_0 = P(\tilde{Y} = 1|Y = 0) = 0$, $e_1 := P(\tilde{Y} = 0|Y = 1)$ is the label noise rate. So here we have $\eta(X) = e_1$, and the expected label error is equal to the label noise rate, that is $\bar{\eta} = \int_X \eta(X) P(X) dX = e_1$. Thus, we could obtain the following theorem based on the Theorem B.1.

THEOREM B.3 (GENERALIZATION ERROR). *With probability at least $1 - \delta$, the generalization error on datasets \tilde{D} is upper-bounded by*

$$R_{\mathcal{D}}(\hat{f}) \leq e_1 + \sqrt{\frac{2 \log\left(\frac{4}{\delta}\right)}{N}} + P(\tilde{Y} \neq \tilde{Y}^*),$$

where $\tilde{D} = \{(X_n, \tilde{Y}_n)\}_{n \in [N]}$ is the noisy dataset, \hat{f} is the classifier trained on the noisy dataset, e_1 is the label noise rate, and \tilde{Y}^* is the prediction of the Bayes optimal classifier f^* .

As the label noise rate e_1 gets smaller, the upper bound for the generalization error of classifier f also decreases when the benefit of label noise rate reduction is more significant than the harm of losing training samples.

C More experiments and discussions

C.1 Additional Studies

Augmentation-based methods. Since our goal is point-level prediction, we adapted augmentation-based methods by assigning anomaly labels to all points within a sample if the sample is predicted as anomalous. We also include segment-level results for reference, even though our focus is point-level prediction using noisy segment-level labels. As shown in Table 9, our method outperforms the others in all three metrics for point-level prediction, which is the focus of our paper. We believe that the performance differences arise due to the different target settings of the three methods and do not necessarily indicate which approach is better or worse.

C.2 Hyperparameters Details

NRdetector is implemented in PyTorch, and some important parameter values used in the proposed method are listed in Table 10. The dimension of the temporal embedding d_{model} is 64. In the process of confidence-based sample selection, we use m to control the number of iterations and use λ_0 to control the size of set to be filtered out. For all datasets, we set $m = 4$ and $\lambda_0 = 0.32$. *batch_size* is set to 32, *learning_rate* is set to $1e - 5$, and *window_size* is 100. *prior* is the estimation of π_P in PU loss (see 4.2.3). *anoamly_ratio* is the predefined point-level anomaly rate in the data-centric point-level detection module.